

Interplay of static and dynamic effects in ${}^6\text{He} + {}^{238}\text{U}$ fusionW. H. Z. Cárdenas,¹ L. F. Canto,² N. Carlin,¹ R. Donangelo,² and M. S. Hussein¹¹*Instituto de Física, Universidade de São Paulo, Caixa Postal 66318, 05389-970 São Paulo, Brazil*²*Instituto de Física, Universidade Federal do Rio de Janeiro, Caixa Postal 68528, 21941-972 Rio de Janeiro, Brazil*

(Received 18 July 2003; published 26 November 2003)

We investigate the influence of the neutron halo and the breakup channel on the total ${}^6\text{He} + {}^{238}\text{U}$ fusion cross section at near-barrier energies. To include static effects of the $2n$ -halo in ${}^6\text{He}$ nuclei, we use a single-folding potential obtained from an appropriate nucleon- ${}^{238}\text{U}$ interaction and a realistic ${}^6\text{He}$ density. Dynamical effects arising from the breakup process are then included through coupled-channel calculations. These calculations suggest that static effects dominate the cross section at energies above the Coulomb barrier, while the coupling to the breakup channel is more important at sub-barrier energies. The comparison of our calculations with recent data suggests that the coupling to other channels may be influencing the cross section at very low energies.

DOI: 10.1103/PhysRevC.68.054614

PACS number(s): 25.60.Pj

I. INTRODUCTION

The recent availability of radioactive beams has made it possible to study reactions involving unstable nuclei [1]. Several of the light neutron- and proton-rich nuclei exhibit halo structures, with a compact core plus one or two loosely bound nucleons. For example, ${}^{11}\text{Li}$ and ${}^6\text{He}$ are two-neutron, Borromean halo nuclei, while ${}^{11}\text{Be}$ and ${}^{19}\text{C}$ are one-neutron halo nuclei. The isotope ${}^8\text{B}$ has been confirmed to have a one-proton halo, while ${}^{17}\text{F}$ is a normal nucleus in its ground state but becomes a one-proton halo in its first excited state. One important feature of these loosely bound systems is that they exhibit the so-called soft giant resonances (pygmy resonances), the most notorious of which is the soft dipole resonance, very nicely confirmed in ${}^6\text{He}$ by Nakayama *et al.* [2].

Reactions induced by these nuclei are important in processes of astrophysical interest, among others. We ask the question of how the above systems fuse, in particular, how the fusion induced by these nuclear species behaves as a function of bombarding energy, especially near the Coulomb barrier.

The main new ingredient in reactions induced by unstable projectiles is the strong influence of the breakup channel. Because of this channel, one may have different kinds of fusion processes. If all the nucleons in the projectile and in the target form a compound system, the process is called *complete fusion*. If only part of the projectile fragments is absorbed by the target, the process is called *incomplete fusion*. The *total fusion* cross section, defined as the sum of complete and incomplete fusion cross sections, is the quantity usually measured in experiments. Theoretical studies [3,4] of the complete fusion process in reactions induced by very weakly bound projectiles, e.g., ${}^{11}\text{Li}$, indicate that the coupling to the breakup channel hinders this cross section at above- and near-barrier energies. However, even in this case the complete fusion cross section is enhanced at sufficiently low energies. On the other hand, in the calculations of Ref. [4] the coupling to the breakup channel is shown to enhance the total fusion cross section below and above the barrier. More recent calculations show that this coupling leads to an

important enhancement of the total fusion cross section at sub-barrier energies and to small effects at energies above the Coulomb barrier [5].

The experimental activities in this area are increasing at a fast rate. To be precise, four such measurements have been published. Signorini *et al.* [6] reported the fusion of ${}^9,{}^{10},{}^{11}\text{Be}$ on ${}^{209}\text{Bi}$ at energies close to the Coulomb barrier. These authors reach the conclusion that in the case of the weakly bound, albeit stable, isotope ${}^9\text{Be}$, the total fusion cross section is found to be significantly reduced at above-barrier energies owing to the coupling to the breakup channel. The cases of ${}^{10}\text{Be}$ and ${}^{11}\text{Be}$ are more subtle to understand. However, the more recent results of Ref. [7] on ${}^6\text{He} + {}^{238}\text{U}$ and of Ref. [8] on ${}^6\text{He} + {}^{209}\text{Bi}$ do indicate that the total fusion cross section is enhanced at sub-barrier energies. This clearly indicates that the size of the system, influenced by the halo, becomes an important feature leading to enhancement of the fusion process at these low energies, and that the breakup hinders it at above-barrier energies. This conflicting effect becomes more pronounced in well developed halo nuclei, such as ${}^{11}\text{Be}$ (one-neutron halo) and ${}^6\text{He}$ (two-neutron halo). We should mention that Signorini *et al.* [6] have further shown that the fusion of the normal, strongly bound, isotope ${}^{10}\text{Be}$ is larger at above-barrier energies than that of the one-neutron halo ${}^{11}\text{Be}$. This is supported by the work of Hinde *et al.* [9] on the fusion of ${}^9\text{Be}$.

The fusion of the proton-rich isotope ${}^{17}\text{F}$ with ${}^{208}\text{Pb}$ was measured by Rehm *et al.* [10]. This weakly bound nucleus has a normal ground state, but its first excited state is mostly $l=0$ and seems to exhibit a halo characteristic. The results of this measurement indicate a rather normal behavior of the complete fusion cross section, with very small effect of breakup, though the breakup channel (${}^{17}\text{F} \rightarrow {}^{16}\text{O} + p$) coupling would result in a lowering of the Coulomb barrier.

Recently, nuclear reactions induced by ${}^6\text{He}$ projectile have attracted considerable interest [11]. In particular, very interesting experimental data on the fusion of He isotopes with ${}^{238}\text{U}$ have been obtained [7]. These data show an enhancement of several orders of magnitude of the ${}^6\text{He} + {}^{238}\text{U}$ total fusion cross section with respect to that of ${}^4\text{He} + {}^{238}\text{U}$. The

physical process leading to this result has not yet been established. A natural candidate is the coupling with the breakup channel (${}^6\text{He} \rightarrow {}^2\text{He} + 2n$). This led us to develop a schematic model to estimate the static and dynamic effects of the breakup channel on the total fusion cross section. Our model takes into account both the Coulomb and the nuclear couplings, within the dipole approximation. This breakup states are approximated by a single effective channel concentrating the full dipole strength.

The paper is organized as follows. The following section describes the calculation of the static effects brought about by the presence of a nuclear halo. The coupling to the breakup channel is performed, by means of schematic coupled-channel calculations, in Sec. III. Our conclusions are presented in Sec. IV.

II. STATIC EFFECTS FROM THE $2n$ -HALO

The weakly bound neutrons in ${}^6\text{He}$ are expected to influence the fusion cross section in two ways. First, by the static effect of barrier lowering due to the existence of a halo. Second, through the coupling with the breakup channel. In this section we consider the first of these effects.

Owing to the two weakly bound neutrons in ${}^6\text{He}$, the nuclear density has a long-range tail and so does the real part of the optical potential describing the ${}^6\text{He}$ -target collision. In this way, the potential barrier is lowered and the fusion cross section is enhanced. In order to account for this effect, we use a single-folding model to describe the real part of the nuclear ${}^6\text{He}$ - ${}^{238}\text{U}$ interaction. This potential is given by the expression

$$V_N(\mathbf{r}) = \int v_{n-T}(\mathbf{r} - \mathbf{r}') \rho(\mathbf{r}') d^3\mathbf{r}'. \quad (1)$$

Above, $v_{n-T}(\mathbf{r} - \mathbf{r}')$ is a phenomenological interaction between a nucleon and the ${}^{238}\text{U}$ target nucleus and $\rho(\mathbf{r}')$ is a realistic ${}^6\text{He}$ density containing the contribution from the halo. The nucleon- ${}^{238}\text{U}$ interaction is obtained from studies of the collision of low-energy neutrons with heavy target nuclei in the actinide region. It can be written as (discarding the spin-orbit part) [12]

$$v_{n-T}(x) = -V_0 f_r(x), \quad (2)$$

with

$$V_0 = \left[50.378 - 27.073 \left(\frac{N-Z}{A} \right) - 0.354 E_{\text{lab}} \right] \text{ MeV} \quad (3)$$

and

$$f_r(x) = \frac{1}{1 + \exp[(x - R_r)/a_r]}, \quad (4)$$

with the parameters $R_r = 1.264 A_T^{1/3}$ fm and $a_r = 0.612$ fm. The total optical potential is then given by

$$U(r) = V_N(r) + V_C(r) - iW(r). \quad (5)$$

Above, $V_C(r)$ is the usual Coulomb interaction in nuclear collisions,

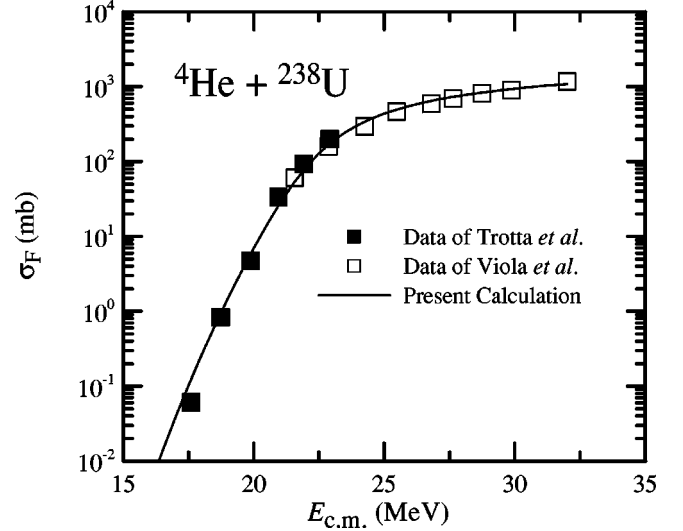


FIG. 1. ${}^4\text{He} + {}^{238}\text{U}$ fusion cross sections. The data of Refs. [7] (solid squares) and [14] (open squares) are compared with the calculations of the present work. The barrier energy is indicated by an arrow. For further details see the text.

$$V_C(r) = \begin{cases} \frac{Z_P Z_T e^2}{r}, & r \geq R_C = 1.2(A_T^{1/3} + A_P^{1/3}) \\ \frac{Z_P Z_T e^2}{2R_C} \left(3 - \frac{r^2}{R_C^2} \right), & r < R_C, \end{cases} \quad (6)$$

and $W(r)$ is a volumetric strong absorption potential with small values for both its radius and diffusivity. We use the parametrization

$$W(r) = W_0 f_i(r), \quad (7)$$

with $W_0 = 50$ MeV and $f_i(r)$ a Wood-Saxon shape as in Eq. (4) with

$$R_i = 1.0(A_P^{1/3} + A_T^{1/3}) \text{ fm}, \quad a_i = 0.10 \text{ fm}. \quad (8)$$

As a test, we applied the above procedure to ${}^4\text{He} + {}^{238}\text{U}$ fusion. The nuclear potential was evaluated by Eq. (1) using a Gaussian density. We write

$$\rho(r) = C \exp(-r^2/\gamma^2) \quad (9)$$

and choose the parameters C and γ so as to give the correct normalization and experimental rms radius. That is,

$$\int \rho(r) d^3r = A; \quad \int r^2 \rho(r) d^3r = A r_{\text{rms}}^2. \quad (10)$$

In the present case, we set $A = 4$ and $r_{\text{rms}} = 1.49$ fm [13]. The fusion cross section obtained with our optical model calculation with the single-folding potential is shown in Fig. 1 (thin solid line), in comparison with the data of Trota *et al.* [7] and the data of Viola and Sikkeland [14]. The agreement is very good. Since this calculation contains no free parameter, this agreement indicates that the procedure is reasonable.

We now consider ${}^6\text{He} + {}^{238}\text{U}$ fusion. First, we disregard the existence of the ${}^6\text{He}$ halo and repeat the above procedure. We

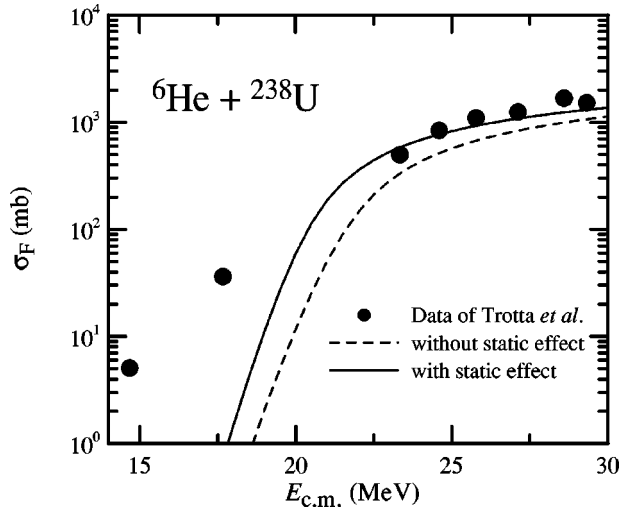


FIG. 2. Coulomb coupling to the breakup channel for the ${}^6\text{He} + {}^{238}\text{U}$ fusion cross section. Experimental results [7] are compared with a static calculation similar to that of Fig. 1, with just a scaling of the potential ${}^4\text{He}$ (dashed line), and taking into account the fact that ${}^6\text{He}$ is a halo nucleus (full line).

parametrize the density as in Eq. (9) and scale the density and rms radius to ${}^6\text{He}$. That is, we set in Eq. (10) $A=6$ and $r_{\text{rms}}=(6/4)^{1/3} \times 1.49$ fm. This density is then used in Eq. (1) and the folding potential is determined. The fusion cross section calculated with this potential is shown in Fig. 2 (dashed line), in comparison with the data [7]. The agreement is poor throughout the considered energy range. We now take into account the existence of the ${}^6\text{He}$ halo, replacing the Gaussian of Eq. (9) by a realistic parametrization [13] of the ${}^6\text{He}$ density, based on the symmetrized Fermi distribution of Ref. [15]. It leads to the rms radius $r_{\text{rms}}=2.30$ fm. Using this density in Eq. (1), we obtain a potential which includes contributions from the ${}^4\text{He}$ core and also from the $2n$ -halo. The resulting fusion cross section is represented by a solid line in Fig. 2. We note that the agreement with the data at above-barrier energies ($E_{\text{c.m.}} > V_B \approx 22.3$ MeV) where c.m. stands for center of mass is considerably improved. Since the Coulomb barrier height is reduced by the attractive contribution from the halo, the cross section becomes larger. However, at sub-barrier energies the agreement remains very poor. The theoretical prediction for the fusion cross section is still several orders of magnitude smaller than the experimental data.

III. COUPLED-CHANNEL EFFECTS

It is well known that the coupling between channels enhances the fusion cross section at sub-barrier energies [16]. Therefore, coupled-channel effects should be taken into account in a theoretical description of the fusion process. However, in the case of coupling to the breakup channel the situation is more complicated since the breakup channel involves an infinite number of continuum states. A possible treatment of the problem is to reduce it to a finite number of channels using the continuum discretization coupled-channel (CDCC) method [17]. This was done in Refs. [5,18] for the fusion of ${}^{11}\text{Be}$ with ${}^{208}\text{Pb}$. However, the present case is much

more complicated since ${}^6\text{He}$ breaks into three fragments instead of two, and the CDCC method has not yet been developed for two-nucleon halo nuclei.

In the present work we use a schematic model to estimate the total fusion cross section. This model is based on two approximations. The first one consists of neglecting the relative motion of the two neutrons in the ${}^6\text{He}$ halo, treating the neutron pair as a single particle. This approximation has led to reasonable descriptions of ${}^{11}\text{Li}$ breakup [19]. On the other hand, it has been criticized in Ref. [20] as it leads to an overestimation of ${}^6\text{He}$ breakup cross section. The second approximation consists of replacing the breakup channel by an *effective channel* [21]. This state has energy equal to the breakup threshold and carries the full strength of the continuum. This procedure is justified when breakup occurs through a low lying, long lived resonance (with a half-life much larger than the collision time), as seems to be the case [2] with ${}^6\text{He}$. Since the kinetic energy of the relative motion between the ${}^4\text{He}$ core and the neutron pair is neglected, this approximation also overestimates the importance of the coupling to the breakup channel. Because of these two approximations, the simplified model of the present work tends to overestimate the role of the breakup channel on the fusion cross section.

The starting point of the coupled-channel method is the Schrödinger equation for the colliding system,

$$H\Psi(\mathbf{r}, \xi) = E\Psi(\mathbf{r}, \xi), \quad (11)$$

where \mathbf{r} is the projectile-target vector, ξ stands for the relevant intrinsic coordinates, E is the total energy in the center of mass frame, and H is the total Hamiltonian of the system.

One then performs the channel expansion of the wave function

$$\Psi(\mathbf{r}, \xi) = \sum_{\alpha} \psi_{\alpha}(\mathbf{r}) \phi_{\alpha}(\xi), \quad (12)$$

where $\phi_{\alpha}(\xi)$ denotes an intrinsic state with energy ϵ_{α} and $\psi_{\alpha}(\mathbf{r})$ is the relative motion wave function in channel α . Substituting this expansion in Eq. (11), we obtain the coupled-channel equations

$$(E_{\alpha} - H_{\alpha})\psi_{\alpha}(\mathbf{r}) = \sum_{\beta} \mathcal{V}_{\alpha\beta}(\mathbf{r})\psi_{\beta}(\mathbf{r}). \quad (13)$$

Above, $E_{\alpha}=E-\epsilon_{\alpha}$ and $H_{\alpha}=T+U_{\alpha}(r)$, where $U_{\alpha}(r)$ is the optical potential in channel α . The channels are coupled through an interaction $\mathcal{V}(\mathbf{r}, \xi)$ with matrix elements in channel space given by

$$\mathcal{V}_{\alpha\beta}(\mathbf{r}) = \int d\xi \phi_{\alpha}^*(\xi) \mathcal{V}(\mathbf{r}, \xi) \phi_{\beta}(\xi). \quad (14)$$

For practical purposes, it is convenient to carry out angular momentum expansions. The wave function is then written as (see, e.g. Ref. [22])

$$\begin{aligned} \Psi^{(+)}(\alpha_0 \nu_0 \mathbf{k}_0; \mathbf{r}) &= \frac{4\pi}{(2\pi)^{3/2}} \sum_{JMl_0} \langle JM | l_0(M - \nu_0) l_0 \nu_0 \rangle \\ &\times Y_{l_0(M-\nu_0)}^*(\hat{\mathbf{k}}_0) \\ &\times \sum_{\alpha l} \mathcal{Y}_{\alpha l}^{JM}(\zeta) \frac{u_{\alpha l, \alpha_0 l_0}^J(k_\alpha, r)}{k_0 r} \end{aligned} \quad (15)$$

and using this expansion in Eq. (11) one obtains the angular momentum projected coupled-channel equations

$$\begin{aligned} \left[E_\alpha + \frac{\hbar^2}{2\mu} \left(\frac{d^2}{dr^2} - \frac{l(l+1)}{r^2} \right) - \mathcal{V}_{\alpha l}^J(r) \right] u_{\alpha l, \alpha_0 l_0}^J(k_\alpha, r) \\ = \sum_{\alpha' l'} \mathcal{V}_{\alpha l, \alpha' l'}^J(r) u_{\alpha' l', \alpha_0 l_0}(k_{\alpha'}, r). \end{aligned}$$

In the present calculation, α takes only the values 0 (elastic channel) and 1 (effective breakup channel). For the energy of the breakup channel we used $\epsilon_1 = 0.975$ MeV, which corresponds to the breakup energy. As mentioned above, this means we neglect the kinetic energy of the relative motion of the fragments after breakup.

We initially consider the coupling interaction as the electric dipole term in the multipole expansion of the electromagnetic interaction between the projectile and the target. This is based on the idea that in order to break a very weakly bound nucleus only a small perturbation is needed. The fact that the breakup cross section for these nuclei is very large suggests that this process is important.

In the case of an electric dipole interaction, the coupling matrix elements are [22]

$$\mathcal{V}_{1l, 0l_0}^J(r) = A i^{l-l_0} \hat{l} \sqrt{\frac{4\pi}{3}} \frac{1}{r_2} \begin{pmatrix} l & 1 & l_0 \\ 0 & 0 & 0 \end{pmatrix} \begin{Bmatrix} J & 1 & l \\ 1 & l_0 & 0 \end{Bmatrix}, \quad (16)$$

with

$$A = eZ_T \sqrt{B(E1, 0 \rightarrow 1)} (-)^{J+1} \quad (17)$$

Above,

$$\begin{pmatrix} l & 1 & l_0 \\ 0 & 0 & 0 \end{pmatrix}$$

and

$$\begin{Bmatrix} J & 1 & l \\ 1 & l_0 & 0 \end{Bmatrix}$$

are the usual $3J$ and $6J$ symbols [23]. Note that the above matrix elements are fully determined, except for the value of the reduced transition probability $B(E1, 0 \rightarrow 1)$.

Solving the coupled-channel equations, one obtains the fusion cross section by the formula [below, the constant $(2\pi)^3$ arises from the normalization factor $(2\pi)^{-3/2}$ in $\psi_\alpha^{(+)}$]

$$\sigma_F = (2\pi)^3 \frac{k_0}{E} \sum_{\alpha=0}^1 \langle \psi_\alpha^{(+)} | W_\alpha | \psi_\alpha^{(+)} \rangle. \quad (18)$$

The method of the present work was used to evaluate the fusion cross section in the ${}^6\text{He} + {}^{238}\text{U}$ collision. We used the optical potential discussed in the preceding section, which includes the static effects of the halo. The coupling matrix elements were given by Eqs. (16) and (17), with $B(E1, 0 \rightarrow 1)$ given by the cluster model [1],

$$B(E1, 0 \rightarrow 1) = \frac{3\hbar^2 e^2}{16\pi \epsilon_1 \mu_{2n-{}^4\text{He}}}. \quad (19)$$

Above, ϵ_1 is the energy binding the *dineutron* to ${}^4\text{He}$ in the ${}^6\text{He}$ nucleus and $\mu_{2n-{}^4\text{He}}$ is the corresponding reduced mass. Taking the numerical value of Eq. (19), we obtain $B(E1, 0 \rightarrow 1) = 1.37 e^2 \text{ fm}^2$.

Recently, Hagino *et al.* [18] have shown that the effects of the nuclear coupling may extend quite far in the case of weakly bound nuclei. In order to estimate the additional dynamic effects arising from the nuclear interaction, we must include the coupling due to the nuclear potential. Since we use an effective channel to describe breakup states, the calculation of the nuclear form factor is a complicated task. For the estimates of the present work, we considered the nuclear interaction potential associated with ${}^6\text{He}$ breakup to be the difference between the sum of the nuclear potentials between ${}^{238}\text{U}$ and ${}^4\text{He}$ and the dineutron, and between ${}^{238}\text{U}$ and the ${}^6\text{He}$ projectile, i.e.,

$$V_{\text{int}}^N(\mathbf{r}, \mathbf{x}) = V_{4\text{He}}(\mathbf{r} + \mathbf{x}/3) + V_{2n}(\mathbf{r} - 2\mathbf{x}/3) - V_{6\text{He}}(\mathbf{r}). \quad (20)$$

Above, \mathbf{x} is the vector going from the dineutron to the ${}^4\text{He}$ cluster, V_{2n} is twice the potential of Eq. (2) and $V_{4\text{He}}$ and $V_{6\text{He}}$ are the folding potentials of the preceding section. We carry out the angular momentum expansion

$$V_{\text{int}}^N = \sum_{\lambda, \mu} Y_{\lambda\mu}(\hat{r}) Y_{\lambda\mu}^*(\hat{x}) V_\lambda^N(r, x) \quad (21)$$

and keep only the dipole term ($\lambda=1$). In this way, the nuclear form factor is

$$F_{\lambda=1}^N(k; r) = \int_0^\infty dr \phi_0(x) V_1^N(r, x) u_1(k, x), \quad (22)$$

where $\phi_0(x)$ is the radial function associated with the bound state of the $2n-{}^4\text{He}$ system and $u_1(k, x)$ is the $l=1$ continuum radial wave function for the same system, with energy $E_k = \hbar^2 k^2 / 2\mu_{2n-{}^4\text{He}}$. Both functions are calculated using the radial Schrödinger equation associated with the internal coordinate \mathbf{x} . The depth of the $V_{2n-{}^4\text{He}}$ potential was set in order to have the second S state with energy $E_0 = -0.975$ MeV (to be consistent with the Pauli principle we discarded the first S state). Owing to the normalization of $u_1(k, x)$, the above form factor vanishes in the $k \rightarrow \infty$ limit. However, the absolute strength of $F_{\lambda=1}^N$ should be treated as a free parameter, since the final state is an effective channel. In this way, we adopt the form factor

$$F_1^N(r) = F_0 f(r), \quad (23)$$

with

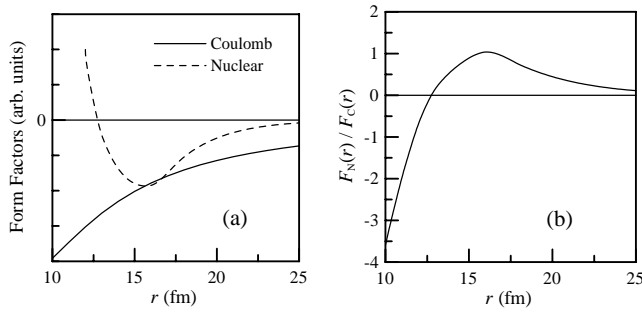


FIG. 3. Coulomb and nuclear dipole form factors (a) and their ratio (b). See text for details.

$$f(r) = \lim_{k \rightarrow \infty} \left[\frac{F_{\lambda=1}^N(k; r)}{F_{\lambda=1}^N(k; 0)} \right]. \quad (24)$$

To estimate the strength F_0 , we adopt the following procedure. First, we evaluate the Coulomb form factor as we evaluated the nuclear one. Instead of using $B(E1, 0 \rightarrow 1) = 1.37 e^2 \text{ fm}^2$, we calculate reduced matrix elements of the dipole term in the Coulomb coupling using the analog of Eq. (22). The resulting Coulomb and nuclear dipole form factors are shown in Fig. 3. Since the dipole term of the nuclear coupling cannot be written as a product of a function of r times a function of x , as can the Coulomb coupling to a good approximation, the shape of the nuclear form factor depends on the energy of the continuum state in the x space. However, the shape of the nuclear form factor does not change much as $k \rightarrow 0$. Although both form factors go to zero in this limit, they decrease by a common factor. In Fig. 3, we show the Coulomb and the nuclear form factors for a very low energy in the continuum. We see that the ratio of these form factors changes strongly with the radial distance. The Coulomb form factor dominates at large separations while the nuclear form factor is larger at small separations. They have approximately the same strength at $r \approx 16$ fm. In the present calculation, we use the experimental $B(E1, 0 \rightarrow 1)$ value and choose the parameter F_0 such that the ratio between the nuclear and the Coulomb form factors is maintained. We should remark that although the nuclear coupling is treated in an approximate way, the present calculation fully contains Coulomb-nuclear interference.

Figure 4 shows the ${}^6\text{He} + {}^{238}\text{U}$ total fusion data in comparison to the static (dashed line) calculation of the preceding section, and two coupled-channel calculations. The thin line is the coupled-channel calculation restricted to Coulomb breakup. We notice that the cross section at high energies is little affected by the inclusion of the breakup channel. Although the sub-barrier cross section is larger than that found in the preceding section, it remains much smaller than the experimental values.

The solid line is the calculation including also the nuclear coupling. We notice that it also changes little the cross section at high energies, and although the nuclear coupling affects more the fusion cross section at sub-barrier energies, the slope remains much larger than that suggested by the

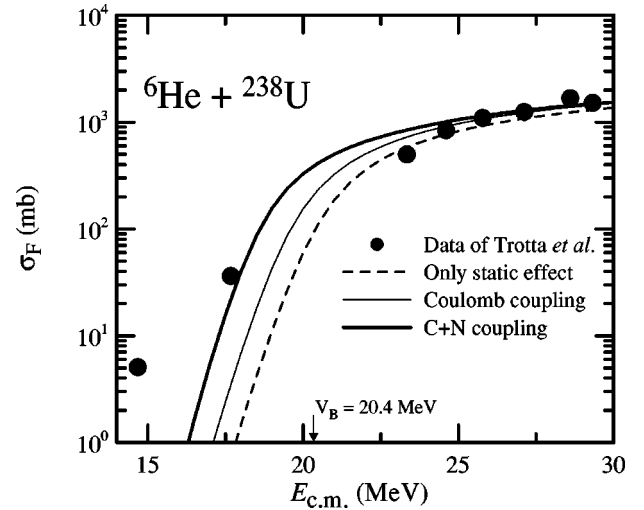


FIG. 4. Total fusion data of ${}^6\text{He}$ incident on ${}^{238}\text{U}$ in comparison to the static calculation, including the ${}^6\text{He}$ halo, of Fig. 2 (dashed line), a coupled-channel calculation including only the Coulomb interaction (thin full line), and also including nuclear effects (thick full line). See text for details on these two last calculations.

data. Changing the strength or diffuseness parameters of this coupling does not change this behavior.

It should be pointed out that the coupling with excited states of ${}^{238}\text{U}$ is not likely to be relevant for this issue, since they were not necessary for the description of the ${}^4\text{He} + {}^{238}\text{U}$ fusion data, considered in Sec. II. As our calculation should provide an upper limit for the cross section, the experimental fusion cross section at the lowest energies cannot be explained through our calculations. However, one should keep in mind that in the calculations presented here we have not included effects due to coupling to channels other than breakup and, in particular, the transfer channels. As transfer close to the optimal Q value may be quite important at sub-barrier energies [24], coupling to these channels, which should not affect much the ${}^4\text{He} + {}^{238}\text{U}$ fusion, is expected to influence strongly sub-barrier ${}^6\text{He} + {}^{238}\text{U}$ fusion. This could also be the case for the ${}^6\text{He} + {}^{209}\text{Bi}$ total fusion cross section where the data [8] show a similar trend as sub-barrier energies.

IV. CONCLUSIONS

We have investigated static and dynamic effects on the ${}^6\text{He} + {}^{238}\text{U}$ fusion cross section. Static effects of the halo were taken into account through the use of an appropriate optical potential. This potential was obtained by the single-folding model, with a nucleon-target interaction which is able to reproduce the ${}^4\text{He} + {}^{238}\text{U}$ fusion cross section and from a realistic ${}^6\text{He}$ density. Our calculations have shown that static effects are important at all collision energies in the range considered. Dynamical effects were considered in a simplified coupled-channel calculation, in which the neutron halo was treated as a dineutron cluster and the breakup channel was represented by a single state with zero energy, concentrating all the low-energy dipole strength. From our calculations we concluded that the static effects dominate the be-

havior of the fusion cross section at energies above the Coulomb barrier and that the coupling to the breakup channel is important mostly below the barrier.

The main conclusion of the present work is that the coupling with the breakup channel cannot, by itself, reproduce the main trends of the data of Trotta *et al.* [7] in the sub-barrier region. This conclusion should not be affected by the simplifying assumptions of our schematic model, since the adopted approximations tend to overestimate the influence of the breakup channel and thus the sub-barrier fusion cross section. As pointed out by Diaz-Torres and Thompson [5], the coupling among the continuum states, which was not included in our schematic model, leads to a reduction of the complete and the total fusion cross sections. This indicates that a full description of the ${}^6\text{He}+{}^{238}\text{U}$ fusion cross section at sub-barrier energies requires the inclusion of neutron-transfer channels.

After the completion of this paper we have learned [25] that the data of Trotta *et al.* [7] have been reanalyzed and

new data with a different experimental setup have been taken. The new set of data seems to indicate that the large enhancement at sub-barrier energies is due to fission induced by neutron transfer rather than fusion-fission events.¹

ACKNOWLEDGMENTS

The authors are grateful to Professor H. D. Marta, from the Instituto de Física, Facultad de Ingeniería, Montevideo, Uruguay, for his help in the calculation of the nuclear form factors. This work was supported in part by CNPq and the MCT/FINEP/CNPq (PRONEX) under Contract No. 41.96.0886.00. L.F.C. acknowledges partial support from the FAPERJ, and M.S.H. and W.H.Z.C. acknowledge support from the FAPESP.

¹We thank Christian Beck and Monica Trotta for drawing our attention to this point.

-
- [1] C. A. Bertulani, L. F. Canto, and M. S. Hussein, *Phys. Rep.* **226**, 281 (1993); C. A. Bertulani, M. S. Hussein, and G. Müntzenberg, *Physics of Radioactive Beams* (Nova Science, New York, 2001); M. S. Hussein, L. F. Canto, and R. Donangelo, *Nucl. Phys.* **A722**, 321c (2003).
 - [2] S. Nakayama *et al.*, *Phys. Rev. Lett.* **85**, 262 (2002).
 - [3] M. S. Hussein, M. P. Pato, L. F. Canto, and R. Donangelo, *Phys. Rev. C* **46**, 377 (1992); L. F. Canto, R. Donangelo, P. Lotti, and M. S. Hussein, *ibid.* **52**, R2848 (1995).
 - [4] N. Takigawa, M. Kuratani, and H. Sagawa, *Phys. Rev. C* **47**, R2470 (1993).
 - [5] A. Diaz-Torres and I. J. Thompson, *Phys. Rev. C* **65**, 024606 (2002); A. Diaz-Torres, I. J. Thompson, and C. Beck, *ibid.* (to be published), nucl-th/0307021.
 - [6] C. Signorini *et al.*, *Eur. Phys. J. A* **5**, 7 (1999).
 - [7] M. Trotta *et al.*, *Phys. Rev. Lett.* **84**, 2342 (2000).
 - [8] J. J. Kolata *et al.*, *Phys. Rev. Lett.* **81**, 4580 (1998).
 - [9] D. J. Hinde *et al.*, *Phys. Rev. Lett.* **89**, 272701 (2002).
 - [10] K. E. Rehm *et al.*, *Phys. Rev. Lett.* **81**, 3341 (1998).
 - [11] T. Aumann *et al.*, *Phys. Rev. C* **59**, 1252 (1999).
 - [12] D. G. Madland and P. G. Young, Los Alamos Report No. LA7533-mb, 1978 (unpublished).
 - [13] G. D. Alkhazov *et al.*, *Phys. Rev. Lett.* **78**, 2313 (1997).
 - [14] V. E. Viola and T. Sikkeland, *Phys. Rev.* **128**, 767 (1962).
 - [15] Yu. N. Eldyhev, V. N. Lukyanov, and Yu. S. Pol, *Sov. J. Nucl. Phys.* **16**, 282 (1973).
 - [16] C. H. Dasso, S. Landowne, and A. Winther, *Nucl. Phys.* **A432**, 495 (1985).
 - [17] M. Kawai, *Prog. Theor. Phys. Suppl.* **89**, 11 (1986); N. Austern, Y. Iseri, M. Kamimura, M. Kawai, G. Rawitscher, and M. Yahiro, *Phys. Rep.* **154**, 125 (1987).
 - [18] K. Hagino, A. Vitturi, C. H. Dasso, and S. Lenzi, *Phys. Rev. C* **61**, 037602 (2000).
 - [19] A. Romanelli, L. F. Canto, R. Donangelo, and P. Lotti, *Nucl. Phys.* **A588**, 71c (1995); H. Esbensen, G. F. Bertsch, and C. A. Bertulani, *ibid.* **A581**, 107 (1995); L. F. Canto, R. Donangelo, and A. Romanelli, *Phys. Rev. C* **53**, 3147 (1996).
 - [20] R. Chatterjee, P. Banerjee, and R. Shyam, *Nucl. Phys.* **A692**, 476 (2001).
 - [21] A. M. S. Breitschaft, V. C. Barbosa, L. F. Canto, M. S. Hussein, E. J. Moniz, J. Christley, and I. J. Thomson, *Ann. Phys. (N.Y.)* **243**, 420 (1995).
 - [22] G. R. Satchler, *Direct Nuclear Reactions* (Oxford University Press, Oxford, 1983).
 - [23] A. R. Edmonds, *Angular Momentum in Quantum Mechanics* (Princeton University Press, Princeton, NJ, 1974).
 - [24] E. Switkowski, R. M. Wieland, and Aa. Winther, *Phys. Rev. Lett.* **33**, 840 (1974).
 - [25] M. Trotta (private communication).